Journal of Thermal Analysis and Calorimetry (2022) 147:12535–12545
https://doi.org/10.1007/s10973-022-11521-2

Pyrolysis of polyester and viscose fiber over ZSM-5: synergistic effect and distribution of products

Hongmei Peng[1,2] · Pingli Li[3] · Qi Yang[1]

Received: 19 July 2021 / Accepted: 16 July 2022 / Published online: 4 August 2022

Abstract

Large amounts of textile wastes are discarded annually, not only polluting the environment but also causing a significant waste of resources. Here, we investigate a pyrolysis treatment that can be used for recycling polyester (PET) and viscose fibers (VFs) that are widely used in textiles to obtain valuable chemicals. Thermogravimetry analysis showed that free radicals generated by VF decomposition caused PET to fracture and depolymerize in the co-pyrolysis (CP) process, resulting in a decrease in the initial temperature (T_i). Pyrolysis–gas chromatography/mass spectrometry (Py-GC/MS) investigation uncovered the fact that the addition of a co-feed influenced the product distribution, that the peak area% values of the products changed significantly in the CP process of PET and VFs, and that the presence of PET significantly decreased the relative content of oxygen-containing products. The experimental peak area% values of phenols and alcohols, acids and esters, aldehydes and ketones, and furans were lower during noncatalytic CP than the values calculated based on the individual pyrolysis of PET or VFs, indicating that cross-reactions occurred between PET and VFs, leading to net deoxygenation. Furthermore, it was revealed that the generation of polycyclic aromatic hydrocarbons in catalytic co-pyrolysis was reduced from 67.11 to 25.71% when ZSM-5 was present, while the production of monocyclic aromatic hydrocarbons (MAHs) increased from 32.87 to 74.27%. These results show that ZSM-5 was beneficial for achieving improved MAHs selectivity.

Keywords Polyester · Viscose · Waste textiles · Synergistic effect · Py-GC/MS

Introduction

The consumption of textiles has risen continuously with the increase in the world's population and the improvement in living standards. In particular, the world fiber consumption was reported to be approximately 105 million tons in 2017 [1]. Due to soaring textile production, a large amount of textile wastes produced by the textile industry have been disposed of annually. To date, scrap textiles (fiber products) are restricted by recycling facilities, recycling systems, separation technology, and other factors and have not been recovered effectively; rather, scrap textiles are incinerated or discarded together with other solid wastes [2, 3]. Thus, the disposal of textile wastes has caused great pollution to the environment [4]. Textile fibers are also regarded as the most prevalent form of microplastics, as they have been discovered in fish, shellfish, and even bottled natural mineral water [5–7]. Thus, along with causing the waste of raw materials, the disposal of waste fibers is an important source of pollution and has caused severe damage to the environment [1].

Textile fibers are broadly classified into two types: natural fibers, which include animal and plant fibers [8], and chemical fibers, which are fabricated from natural or synthetic polymers through chemical processing and are also known as man-made fibers, which include regenerated cellulose fibers and synthetic fibers [8, 9]. Polyethylene terephthalate (PET) fiber is a synthetic fiber that is commonly known as polyester and has been widely used due to its excellent fiber-forming properties, mechanical properties, and low cost [10]. It is the most important chemical fiber in global fiber production and has a market share of 70% in the total synthetic fibers industry [11]. Polyester is widely used as a civil engineering material and as

✉ Qi Yang
cdbs123@yeah.net

[1] College of Polymer Science and Engineering, The State Key Laboratory for Polymer Materials Engineering of Sichuan University, Chengdu, China

[2] Chengdu Textile College, Chengdu, China

[3] Sichuan Fire Research Institute of MEM, Chengdu, China

an industrial fabric. Due to its extensive application in textiles, PET microfibers have been found in almost all environmental waters [11, 12]. The nonbiodegradability of synthetic fibers poses a threat to the environment, while at the same time failure to recycle these fibers is a waste of petroleum resources [13]. Viscose fibers (VFs), which are the main variety of regenerated cellulose fibers, are fabricated from natural cellulose materials, such as wood pulp [14]. Viscose fibers have become a substitute for polyester fibers made from petrochemical raw materials and also for cotton fibers that face severe production and geographical constraints. VFs have good hygroscopicity and dyeing properties, and the finished fabric is soft to touch, comfortable to wear, and can be easily processed into textiles, leading to their wide use in the textile industry [15, 16]. Currently, viscose fibers rank third in usage among global fiber products [14].

Of the fabrics widely used in daily life, few are made of pure VF or pure PET; rather, most fabrics are VF/PET blends. Textile wastes are quite heterogeneous due to their different forms and proportions, which limits the recycling of textile wastes [1, 17]. An alternative promising method for the processing of blended fabrics is pyrolysis. Pyrolysis is the direct heating of raw materials in an oxygen-free or anoxic atmosphere that can convert waste into small molecular products such as fuel oil and chemical raw materials to achieve resource recycling [18–20]. When used for the recycling of textiles, pyrolysis can reduce the harm to the environment posed by waste and alleviate the global energy crisis to some extent.

Biomass is a plant resource composed of organic carbon, and it is currently the only renewable resource that can be used for the preparation of liquid fuels [21]. Lignocellulosic biomass is one of the most abundant types of biomass on Earth, and its main components include cellulose, hemicellulose, and lignin [22]. Therefore, viscose fibers are also a kind of biomass. Generally, the bio-oil derived from biomass pyrolysis (without catalyst or modification) has a high oxygen content, low pH value, and low heating value and cannot be directly used in the chemical industry [23, 24]. It is critical to employ appropriate upgrading techniques to increase the quality of bio-oil obtained from biomass pyrolysis [25]. Co-pyrolysis (CP) is the pyrolysis of multiple raw materials having different compositions and properties that takes advantage of the synergistic effect between the molecules in the original materials. In general, CP can boost the yield and quality of pyrolysis oil, as well as its calorific value. A large number of studies have shown that hydrogen-rich petroleum-based polymers donate hydrogen in-situ during CP with biomass, causing free radical interactions and in situ deoxidation, thus improving the quality of the bio-oil [18, 19, 26]. When a biomass–plastic mixture is processed by co-pyrolysis, the interactions between the volatiles from the two different raw materials and between pyrolysis volatiles and solid raw materials promote synergy [27].

The co-pyrolysis of petroleum-based plastics and biomass without a catalyst has the disadvantage of non-selectivity of products and the need for high temperatures. Catalytic co-pyrolysis (CCP) introduces the use of a catalyst in CP. The use of a catalyst can improve the distribution width of the product components to a certain extent and can also reduce the pyrolysis temperature and energy consumption [28]. Zeolites have long been utilized as acidic catalysts in the pyrolysis of liquid fuels due to their distinctive pore structures and chemical characteristics [29, 30]. Among various zeolites, the ZSM-5 catalyst is the most attractive due to its efficient deoxygenation and dehydration capabilities [28]. The CCP of biomass and plastics over ZSM-5 has been extensively studied. Using the HZSM-5 zeolite as a catalyst, Dorado et al. [31] examined into the CCP of different types of biomass and plastics. They found that compared to the pyrolysis of biomass or plastics alone, CCP showed improved selectivity for aromatic compounds. The activation energy of macroalgae and HDPE co-pyrolysis was dramatically lowered in the presence of HZM-5, and the quantities of acids and oxygenated compounds were greatly reduced, according to Xu et al. [32]. He et al. [30] conducted ex-situ CCP of corn stalk (CS) and high-density polyethylene (HDPE) over the HZSM-5 catalyst. They discovered that benzene, toluene, and xylenes were the most common aromatics generated during the CCP process because to the strong shape selectivity of HZSM-5.

The recycling of textile wastes is of great significance for environmental protection and resource conservation. As mentioned above, biomass-based VFs and petroleum-based PET may have great potential in co-pyrolysis conversion to fuel oil. However, there have been few studies on the co-pyrolysis of polyester/viscose. In this work, CCP treatment of commonly used polyester and viscose textile fibers under the action of ZSM-5 was studied for the first time. The thermal decomposition behaviors of PET, VF, and their mixtures were analyzed by thermogravimetry (TG), and the pyrolysis products of PET, VF, and their mixtures were studied by pyrolysis–gas chromatography/mass spectrometry (Py-GC/MS). To evaluate the synergistic effect of VF and PET, the discrepancies between the experimentally measured values and the calculated values of mass loss and pyrolysis products were used. The interactions between the reaction intermediates produced by the pyrolysis of PET and VFs were also analyzed. The results of this work will be beneficial for the future development of methods to increase the selectivity for valuable aromatics in the CCP conversion of textile wastes.

Table 1 Ultimate and proximate analysis of VF and PET

Samples	VF	PET
Ultimate analysis/mass%		
C	43.3	63.0
H	6.2	4.2
O[a]	50.5	32.8
N	–	–
Proximate analysis/mass%		
Moisture	9.69	1.63
Volatile matter	83.26	88.16
Ash	1.15	2.54
Fixed carbon[a]	5.90	7.67

[a]By difference

Materials and methods

Materials

PET granules having an intrinsic viscosity of 0.64–0.66 dL g^{-1} were provided by Sinopec Yizheng Chemical Fiber Co., Ltd. (China). PET granules were melt spun into 38 mm staple fibers with a linear density of 1.66 dtex, by referring to the preceding report for the melt spinning procedure [33]. Viscose fibers were kindly supported by Yibin Grace Co., Ltd. (Chengdu, China). Wet spinning was used to create the VFs, which have an α-cellulose content of 94% and a degree of polymerization of 360–400. Previous papers have documented VF regeneration and wet spinning processes [9, 34]. VFs and PET were decimated into powder using an airflow crusher, and then dried for usage. The data of the proximate and ultimate PET and VF analyses, which were carried out using an elemental analyzer (Euro Vector EA3000, Italy) and in compliance with Chinese National Standards (GB/T 28,731–2012), are presented in Table 1.

The ZSM-5 ($SiO_2/Al_2O_3 = 34$) zeolite catalyst was purchased from Shanghai Ziyi Reagent Factory (Shanghai, China). The catalyst was calcined at 550 ℃ in a muffle furnace, activated for 4 h, cooled, and sealed for storage prior to the catalytic pyrolysis experiments.

Thermogravimetric analysis (TGA)

The thermal degradation behaviors and mass transfer rate of PET, VF, and their mixture (PET/VF:1/1) with and without the catalyst were investigated using a Q500 thermogravimetric analyzer (TA Instruments, USA). In an alumina crucible, about 8–10 mg feedstock was placed and blanketed by nitrogen at a flow rate of 50 mL min^{-1}. Different heating rates of 10, 20, 30, and 40 ℃ min^{-1} were utilized to raise the temperature from room temperature to 750 °C. In the catalytic TG experiments, identical amounts of ZSM-5 catalyst (4 mg) were thoroughly mixed with the samples (PET, VF, or PET/VF) in an agate mortar and then heated under the same conditions as those for the non-catalytic TG experiments. To ensure that the results were accurate and reliable, each experiment was repeated three times.

Kinetic analysis

The thermal degradation of these materials is a complex physicochemical process involving chemical reactions, physical changes, and heat and mass transfer [35]. The design of such a complex pyrolysis process for a material depends essentially on kinetic analysis. Kinetic parameter data are important for understanding the thermochemical conversion. In this paper, the Kissinger–Akahira–Sunose (KAS) method was used to estimate the reaction's activation energy (E) using TGA data. The KAS equation is expressed as [32]:

$$\mathrm{In}\left(\frac{\beta}{\mathrm{T}^2}\right) = \mathrm{In}\left[\frac{AR}{Eg(\alpha)}\right] - \frac{E}{RT} \quad (1)$$

where β is the heating rate (K min^{-1}), T is the absolute temperature (K), $g(\alpha)$ is the integrated form of the reaction mechanism function, A and E are the pre-exponential factor (s^{-1}) and the apparent activation energy (kJ mol^{-1}), respectively, and R is the universal gas constant (8.314 J mol^{-1} K^{-1}). α is the amount of material that has been pyrolyzed or the percentage of total material that has been converted, and it can be described using the following formula.

$$\alpha = \frac{W_0 - W_t}{W_0 - W_\infty} \quad (2)$$

where W_0 is the initial sample mass, W_t is the sample's mass at time t, and W_∞ is the sample's final mass.

The plot $\mathrm{In}\left(\frac{\beta}{T^2}\right)$ vs. $\frac{1}{T}$ should be a straight line, and E can be evaluated from the slope.

Py-GC/MS analysis

The pyrolytic analysis (Py) experiments were carried out in a Pyroprobe 5200 instrument (CDS Analytical, USA). In all pyrolysis experiments, the temperature was rapidly raised to 700 ℃ at a flash heating rate of 20 ℃ ms^{-1} and maintained for 60 s. The pyrolysis volatiles entered the adsorption trap (280 ℃, where they were adsorbed for 2 min and then desorbed). High-purity helium gas (99.999%) purged the volatiles generated by heat through the transfer pipeline (280 °C) to the injection port of a gas chromatograph (GC) (GC-450, Varian, USA) equipped with an online mass spectrometer (MS) (240-MS, Varian, USA). Nonpolar CP Si1 8 CB capillary (30 m × 0.32 mm × 0.25 um) was used for GC. The helium carrier gas flow was 1 mL min^{-1} with a split ratio of 20:1. The inlet temperature was 50 °C. The chromatographic column was programmed to carry out the following heating protocol: hold at 40 ℃ for 5 min, then raise the temperature to 300 ℃ at a heating rate of 10 ℃ min^{-1}, and then hold at this temperature for 10 min. MS utilized electron ionization (EI) at 70 eV, had a scan mass range of 40–500 m/z, and an ion source temperature of 230 °C.

In all pyrolysis experiments, samples of PET, VF, and their mixture (PET/VF:1/1) were placed in a 25-mm-long quartz tube (2.0 mm i.d.) and fixed with quartz wool on both ends. Catalytic pyrolysis studies were carried out by placing raw material (about 1 mg) in the middle of a quartz tube and ZSM-5 catalyst (1 mg) on both sides of the quartz tube. The feedstock and catalyst were separated by quartz wool as shown in previous work [21].

The chemical compositions of pyrolysis products were determined according to the relevant literature and the NIST database. To establish reproducibility, all pyrolysis experiments were repeated at least three times. For the GC/MS spectrum obtained in each experiment, each of the products was analyzed in detail, and their relative percentage values and absolute peak areas were recorded (Supplementary materials). The averages of the values obtained in three experiments were used as the final determination values.

Results and discussion

Characterization of materials

Table 1 shows the physicochemical parameters of PET and VFs. PET had a substantially higher total carbon and hydrogen content (67.2 mass%) than VFs (49.5 mass%). This is because VFs have a high oxygen content (50.5 mass%). The high oxygen content that comes from thermochemical conversion methods such as pyrolysis endangers both the calorific value and stability of bio-stability oil [32]. The fact that the structure of the VF contained oxygen-containing functional groups and compounds, such as cellulose, hemicellulose, and lignin, all contributed to the high oxygen concentration that was present in the material [36]. Aromatic rings, esters, and carboxyl groups are all present in PET, contributing to the material's high carbon content and low hydrogen concentration. Similar to the theoretical values for pure PET (C, 62.5 mass%; H, 4.2 mass%; O, 33.3 mass%), the percentages of C, H, and O in PET were 63.0, 4.2, and 32.8 mass%, respectively.

The proximate analysis revealed that both VFs and PET had a significant quantity of volatile matter content (83.26 mass% and 88.16 mass%, respectively), indicating that pyrolysis can release a significant amount of useful products (fuels or gases) [37]. However, PET (2.54 mass%) has a larger ash concentration than VF (1.15 mass%). Caking and scaling are caused by ash, which restricts mass and heat transport [36]. As a result of the aforementioned examination of the basic properties of PET and VFs, it is clear that their independent pyrolysis has limitations. As a result, the

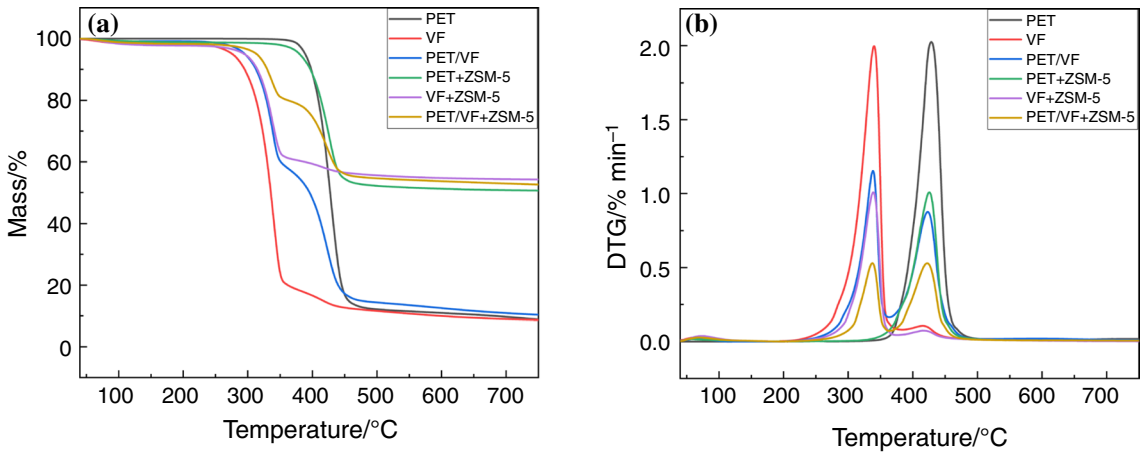

Fig. 1 Thermal and catalytic TG (**a**) and DTG (**b**) curves of PET, VF, and PET/VF composites

Table 2 Thermal parameters of PET, VF, and PET/VF composites with ZSM-5

Sample	Catalyst	The first stage			The second stage		
		T_i/℃	T_{max}/℃	T_f/℃	T_i/℃	T_{max}/℃	T_f/℃
VF	No	258.8	340.1	353.4	–	–	–
	ZSM-5	254.8	338.9	352.8	–	–	–
PET	No	–	–	–	365.2	428.6	453.0
	ZSM-5	–	–	–	358.9	425.6	448.5
PET/VF	No	267.5	338.4	362.4	362.4	423.1	448.9
	ZSM-5	293.1	337.4	363.7	363.7	422.4	450.5

T_i: temperature for initial mass loss, T_{max}: temperature for the maximum mass loss rate, T_f: temperature for final mass loss

synergistic interaction between the two components is critical for improving pyrolysis product quality and yield.

Thermogravimetric analysis

Thermal degradation behaviors and kinetic analysis

The mass loss (TG) and derivative mass loss (DTG) curves of PET, VF, and their blends pyrolysis at a heating rate of 10 °C min^{-1} are displayed in Fig. 1. As presented in Table 2, the main temperature range for VF deterioration was 259–353 ℃, with a maximum mass loss rate at 340 °C. This corresponds to the temperature range of cellulose decomposition [38]. Above 400 °C, the breakdown of the lignocellulosic part of biomass resulted in a gradual loss of mass [39]. Active pyrolysis is the quick decomposition of lignocellulosic biomass below 400 °C, while passive pyrolysis is the sluggish decomposition over 400 °C [40]. The thermal degradation of PET occurred between 365 and 453 °C, with the largest degree of thermal degradation occurring at 429 °C. In the presence of the ZSM-5 catalyst, the cracking temperature ranges shifted to lower temperatures for both PET and VF. This result confirmed that the catalyst significantly reduced the decomposition temperatures [41]. This is in accordance with previous research, which demonstrated that the catalyst can lower the reaction's activation energy, lowering the decomposition temperature [42].

The PET/VF TG and DTG curves were not the same as those of the pure feedstocks. The co-pyrolysis of PET/VF was separated into two steps based on the DTG profile. The first step started at 267–362 ℃, corresponding mainly to the decomposition of the VF, and the second step was between 362 and 449 ℃, mainly due to the decomposition of the PET. The initial temperature (T_i) of the VF increased during co-pyrolysis, while the T_i of PET decreased. This is because when the VF began to degrade, the softened PET covered the VF surface, preventing volatile chemicals from being released [43]. The lower T_i of PET during the co-pyrolysis indicates that VF decomposition products accelerated the PET decomposition and further demonstrates the synergistic effect during the co-pyrolysis of VF and PET. Breakdown of VF produces free radicals, which in turn cause the fracture and depolymerization of PET, accelerating its decomposition and lowering its T_i. According to the findings of Wang et al. [44], the CP of lignin and polyethylene led to the same result. Specifically, the T_i value of the lignin increased while the T_i value of the polyethylene decreased when compared to the T_i values of lignin and polyethylene that were derived from separate pyrolysis.

Table 3 Averaged apparent activation energy of samples determined by KAS

	PET	VF	PET/VF	PET/VF/ZSM-5
$\overline{E}$/kJ mol^{-1}	235.55	169.11	210.46	175.15
R^2	0.9976	0.9969	0.9871	0.9890

Table 3 presents the averaged apparent activation energy ($\overline{E}$) values and the correlation coefficient (R^2) values obtained by the KAS method. The fact that the R^2 values for the broad conversion range (0.1–0.9) were close to 1 (> 0.95) (Table S1) demonstrates that the TGA data had strong fitting capabilities, and it also demonstrates that the activation energy estimations were accurate. The KAS determined that the $\overline{E}$ values for the PET, VF, and PET/VF samples were 235.55, 169.11, and 210.46 kJ mol^{-1}, respectively, as shown in Table 3. When catalytic co-pyrolysis was carried out, the $\overline{E}$ value decreased drastically to 175.15 kJ mol^{-1}, which confirmed that ZSM-5 had an obvious effect on reducing the apparent activation energy.

The synergetic effect of PET/VF blends

Changes in decomposition temperature during the CP process show that VF and PET have a synergistic impact. To further validate the link between the VF and PET samples, theoretical TG/DTG curves were calculated. These curves represent the sum of the individual component behaviors in

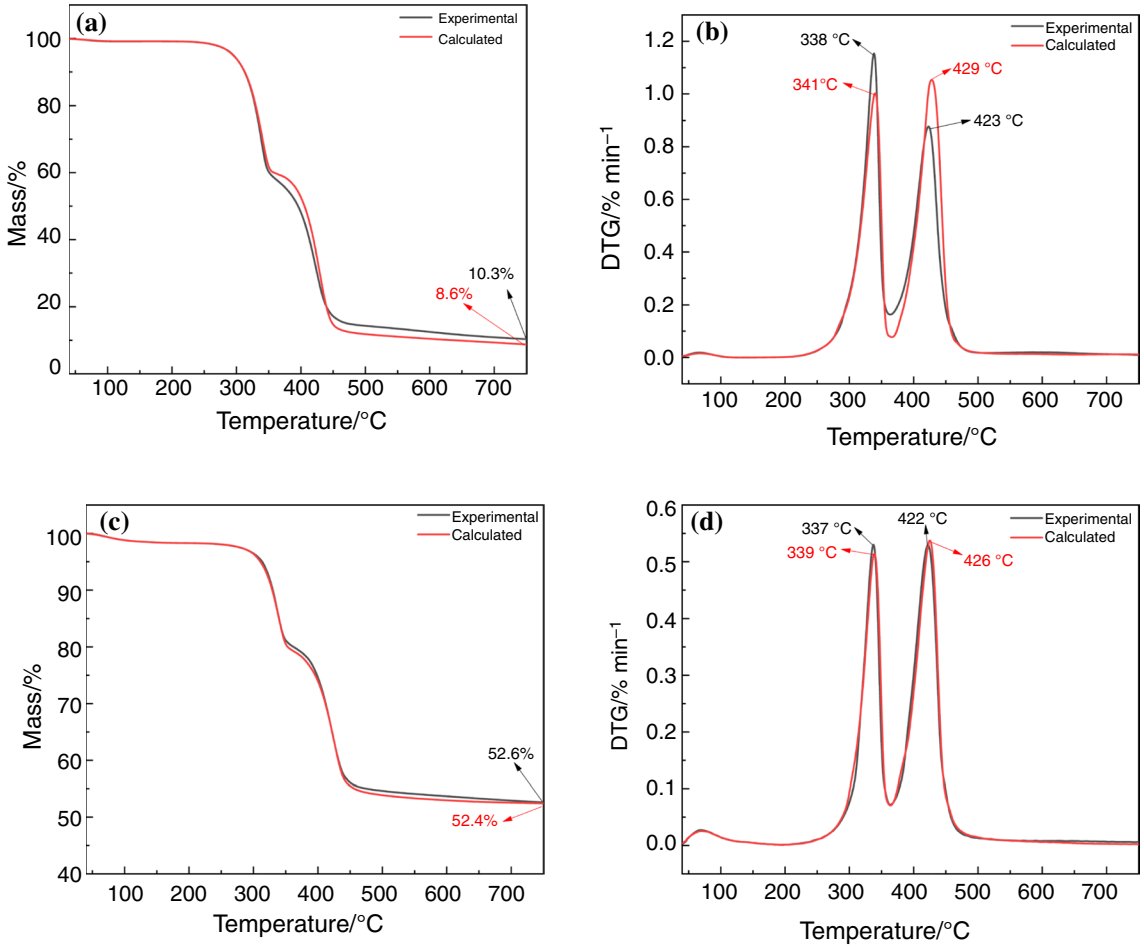

Fig. 2 Experimental and calculated TG and DTG curves of pyrolysis of components (**a** and **b** for PET/VF; **c** and **d** for PET/VF/ZSM-5)

the mixture. The formula for calculating the mass loss values of the mixes is as follows [45]:

$$W_{\mathrm{Cal}} = X_{\mathrm{V}} \bullet M_{\mathrm{V}} + X_{\mathrm{P}} \bullet M_{\mathrm{P}} \tag{3}$$

where W_{Cal} (%) represents the estimated mass percentage of the blends, X_{V} and X_{P} represent the mass fractions of VF and PET in the blend, and M_{V} (%) and M_{P} (%) represent the mass percentage values of the materials in the individual pyrolysis experiments, respectively.

The theoretical and experimental curves are illustrated in Fig. 2. Figure 2a, b shows that the temperature of the first peak (338 ℃) of the experimental DTG curve of the PET/VF mixture was slightly lower than that of the calculated curve (341 ℃), which can be explained by the intermolecular reaction between the pyrolytic molecules [46]. The interaction between VF and PET in the co-pyrolysis process influenced the temperature of the maximum mass loss rate, implying a synergistic effect. The experimental carbon residue value at 750 °C was greater than the corresponding calculated value, suggesting that a substantial amount of solid residue was generated as a result of the interaction between the PET/VF pyrolysis intermediates, as shown in Fig. 2a. Park et al. [47] came to the same result. They found that the amount of residual coke produced experimentally during the co-pyrolysis of Quercus variabilis and waste plastic films was greater than the theoretical yield. When ZSM-5 was added (Fig. 2c), the experimental value of solid residues at 750 ℃ was almost equal to the theoretical value. This indicates that the catalyst can produce more volatile products and reduce the formation of solid residues. During CCP (Fig. 2d), the peak height of DTG in the PET decomposition region was significantly different from that during CP. That is, PET decomposition was accelerated by the catalyst.

Table 4 Main pyrolysis compound obtained from PET, VF, and PET/VF mixture with and without ZSM-5

Compound	Peak area/%					
	PET		VF		PET/VF	
	No cat	ZSM-5	No cat	ZSM-5	No cat	ZSM-5
MAHs	9.43	60.43	16.75	43.73	19.56	61.49
PAHs	24.76	24.22	22.02	42.82	39.92	21.28
Phenols and alcohols	3.50	0.59	24.12	3.87	7.16	3.29
Acids and esters	58.94	11.81	20.27	5.58	29.87	9.82
Aldehydes and ketones	3.37	2.95	6.95	1.09	2.58	–
Furans	–	–	9.90	2.92	0.92	4.12

Py-GC/MS measurement

Product distributions in the pyrolysis of PET, VF and their mixture

Table 4 shows the product distributions obtained in the non-catalytic and catalytic pyrolysis of PET, VF, and their mixture. The identified products were classified into monocyclic aromatic hydrocarbons (MAHs), polycyclic aromatic hydrocarbons (PAHs), phenols and alcohols, acids and esters, aldehydes and ketones, and furans. In the non-catalytic pyrolysis (NCP) of PET, the peak area% values of MAHs and PAHs were 9.43% and 24.76%, respectively. Low contents of aldehydes and ketones were obtained (only 3.37%) that were dominated by benzaldehyde and phenylacetaldehyde. Phenols and alcohols accounted for 3.5%, with phenol as the main component. Meanwhile, the peak area% values of acids and esters reached 58.94%, of which benzoic acid and benzoates made the largest contributions. In the PET degradation process, carboxyl and vinyl terminal groups were formed by the cleavage of the ester bond transferred from β-hydrogen to carbonyl carbon, and then, the C–H bond and C–O alkoxy bond were partially dissociated to form the C=C and O–H bonds [48].

The oxygen-containing compounds produced in VF pyrolysis are mainly acids, esters, ketones, furans, alcohols, phenols, and aldehydes. The content of phenols was 14.45% and was mainly generated by the decomposition of lignin [49]. The main acids and esters were phenacyl formate and methyl pyruvate, with a content of 20.27%. The relative content of aldehydes and ketones was 6.95%, which mainly consisted of compounds such as butanediol, 1,3-cyclopentanedione, 2H-pyran-2,6(3H)-dione, 2-cyclopentene-1,4-dione, methyl cyclopentenolone, 3-methyl-1,2-cyclopentanedione, and levoglucosenone. The main components of furans included furfural, 2-furanmethanol, 2,5-dimethyl-4-hydroxy-3-furanone, and 2-ethyl-5-methylfuran. During the CP of PET and VFs, the values of the peak area% of the products changed greatly, demonstrating that the incorporation of PET significantly reduced the relative amounts of oxygen-containing products.

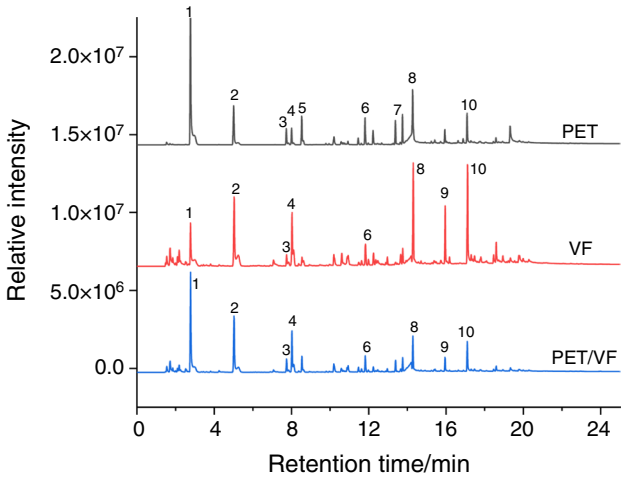

Fig. 3 Ion chromatograms from CP of PET, VF and PET/VF mixture over ZSM-5. (1. benzene; 2. toluene; 3. ethylbenzene; 4. xylene; 5. styrene; 6. p-tolyacetylene; 7. benzoic acid; 8. naphthalene; 9. 2-methylnaphthalene; 10. biphenyl.)

Compared to NCP, catalytic pyrolysis over ZSM-5 produced more hydrocarbons, i.e., MAHs and PAHs, while the fractions of all oxygenated compounds were significantly reduced, indicating that ZSM-5 can promote the deoxygenation of pyrolysis products. Following deoxygenation, the compounds containing oxygen underwent transformations known as oligomerization, cyclization, and hydrogen transfer, which resulted in the formation of aromatic hydrocarbons [50]. Small amounts of oxygen-containing compounds still remained after catalytic pyrolysis, which may be related to the pore size of ZSM-5. It has been noted that the reduced pore size of ZSM-5 precludes bigger oxygen-containing molecules from penetrating the pores and forming aromatic hydrocarbons [29].

Figure 3 compares the ion chromatograms generated by the pyrolysis of PET, VF, and their 1:1 mixture over the ZSM-5 catalyst. As shown in Fig. 3, the main catalytic products were benzene (1), toluene (2), ethylbenzene (3),

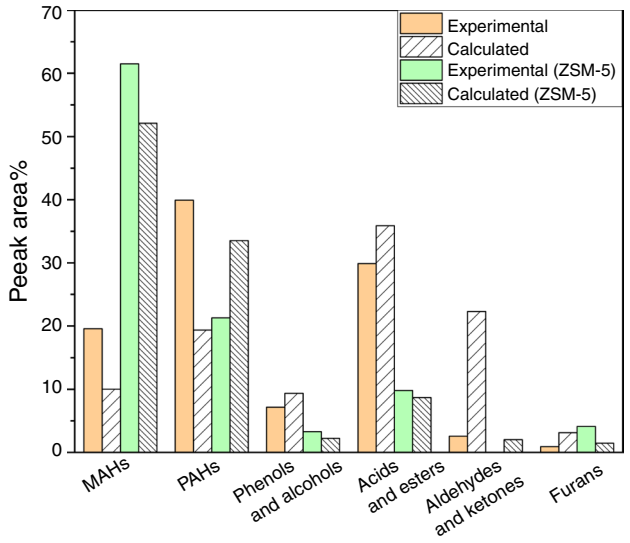

Fig. 4 Relative contents from non-catalytic and catalytic pyrolysis of PET/VF (experimental) and individual pyrolysis of PET and VF (calculated)

xylene (4), styrene (5), naphthalene (8), methylnaphthalene (9), and biphenyl (10). According to the TG results, the co-pyrolysis of PET and VF reduced the decomposition temperature of PET. Comparison of the chromatograms shows that the CCP products were similar to those obtained by the CP of PET and VF alone. This showed that the CCP of PET and VF changed the decomposition temperature but did not change the decomposition mechanism. The product distribution changed with the introduction of a co-feed for CP. Benzoic acid (7) was present in the pyrolysis products of PET, but its content decreased significantly during CCP, indicating that the synergistic effect between PET and VF involves decarboxylation or de-carbonylation. It should be noted that the total hydrocarbon content (MAHs and PAHs) increases strongly during CP and CCP. Consistent with previous reports, the aromatic yield of the biomass/polymer mixture was higher than those of the individual feedstocks [31].

Synergistic effect analysis by Py-GC/MS

Using Py-GC/MS, the synergies between PET and VFs were further explored. The measured pyrolysis product distribution of the PET/VF mixture is referred to as the "experimental" value, and the "calculated" value is the simple linear sum of the independent pyrolysis distributions, which is similar to the calculation of W_{cal} described in the TG experiments. As shown in Fig. 4, a significant difference was observed between the experimental peak area% and the calculated peak area% values.

For phenols and alcohols, acids and esters, aldehydes and ketones, and furans, the experimental peak area% values were lower than the estimated values for non-catalytic CP, indicating that cross-reactions occurred between the PET and VFs, leading to a net deoxygenation. It is well known that the presence of oxygenated compounds has a strong negative impact on the stability of pyrolysis oil, which reduces its value. Co-pyrolysis of biomass and polymers has been shown in numerous investigations to have a synergistic impact. This reduces the production of oxygen-containing compounds and improves the quality of the pyrolysis oil. For example, Lin et al. [51] discovered that the peak area and peak area% values of oxygen-containing compounds such as aldehydes, ketones, and furans were lower than calculated during the co-pyrolysis of poplar wood and polypropylene (PP). This proved the presence of a synergistic effect between poplar wood and PP.

The cross-deoxidation reactions between PET and VFs are highly important because the oligomerization of oxygen-containing pyrolysis intermediates in the biomass can easily form coke, resulting in the reduction in the pyrolysis yield and catalyst deactivation. Under the action of PET derivative intermediates, the oxygen-containing intermediates can be effectively converted into aromatic hydrocarbons to prevent coke formation [52]. In addition, aldehyde and ketone products were no longer obtained by CCP. This can be explained by the fact that hydrogen-rich compounds derived from the polymer can provide hydrogen for biomass oxygenated molecules, so increasing the deoxidation of these compounds and producing light olefins within the pores of the zeolite. A sequence of processes can convert light olefins into aromatic hydrocarbons [53]. In contrast, the experimental contents of other oxygen-containing compounds like phenol and furan were found to be greater than the comparable estimated values. This finding may have some connection to the hydrogen transferability of the ZSM-5 catalyst. Hydrogen was extracted from the PET and transferred to biomass free radicals to produce more oxygen-containing compounds, but these compounds do not diffuse into the pores of ZSM-5 because the size of these molecules is greater than the size of ZSM-5 pores. Lin et al. [29] also reached a similar conclusion in their experiments on the pyrolysis of wood-plastic composites catalyzed by HZSM-5 and discovered that the amounts of phenols and ketones observed in the experiment were significantly higher than the corresponding estimated values. During the CCP, the experimental peak area% values of the MAHs were greater than the estimated values, whereas the experimental peak area% values of the PAHs were less than the calculated values, indicating that the catalyst was more favorable for obtaining higher-value MAHs that can be used as a fuel additive under ambient pressure and do not require an additional hydrogen supply.

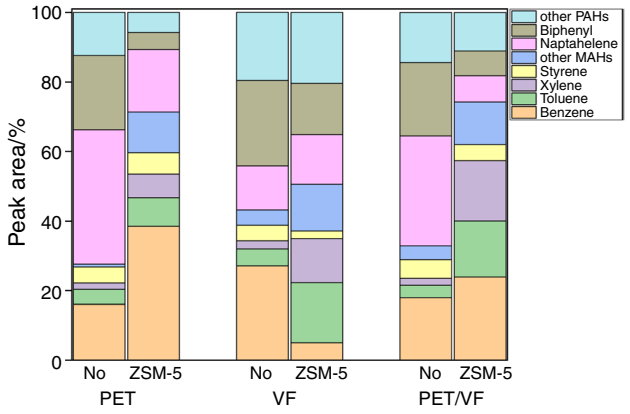

Fig. 5 Aromatics selectivity from the pyrolysis of PET, VF, and their mixture with and without ZSM-5

Aromatics selectivity in Py-GC/MS

MAHs such as toluene, ethylbenzene, and xylene are traditional petroleum derivatives and basic materials for the fuel and chemical industry, and PAHs such as naphthalene and biphenyl are widely used in the production of pesticides, dyes, and other chemicals [31]. The results for the aromatic selectivity in the pyrolysis of PET, VF, and their mixture with and without ZSM-5 are shown in Fig. 5. During fast pyrolysis, the main pyrolysis products usually undergo a hydrocarbon pool mechanism and phenolic pool mechanism at the acid sites of ZSM-5, where alkylation and hydrogen transfer reactions are carried out to generate MAHs and PAHs [54]. Compared to non-catalytic pyrolysis, more MAHs were produced during catalytic pyrolysis. With smaller dynamic particle sizes, ZSM-5 zeolite exhibits strong selectivity for benzene, toluene, xylene, and styrene [55]. In addition, when CCP was applied, the production of PAHs was significantly reduced from 67.11 to 25.71%, while the production of MAHs increased from 32.87 to 74.27% (Table S3). These results show that the use of the ZSM-5 catalyst was beneficial for obtaining enhanced selectivity for MAHs.

Conclusions

In this study, the synergistic effect and pyrolysis product distributions of polyester and viscose fiber over ZSM-5 were investigated via TG and Py-GC/MS for the first time. There was an increase in the T_i value of VF when it was co-pyrolyzed with PET, which indicates that VF degradation products accelerate PET degradation. The interaction between VFs and PET was shown to alter the maximum mass loss rate temperature in the actual and anticipated TG and DTG curves. The Py-GC/MS results show that the peak area% values of the products changed considerably during the CP of PET and VF, with the presence of PET significantly reducing the relative amounts of oxygen-containing products. Compared to NCP, catalytic pyrolysis over ZSM-5 produced more hydrocarbons, while the amounts of the oxygen-containing products were significantly reduced. Benzoic acid was present in the pyrolysis products of PET, but its content decreased significantly during CCP, indicating that the synergistic effect between PET and VF led to decarboxylation or de-carbonylation. For non-catalytic CP, the experimental peak area% values of phenols and alcohols, acids and esters, aldehydes and ketones, and furans were lower than the values calculated from the results of the individual pyrolysis of PET and VF, suggesting that cross-reactions occurred between PET and VF, leading to some net deoxygenation. The CCP results showed that the ZSM-5 catalyst was conducive to obtaining higher-value MAHs. By exploring the benefits of the co-pyrolysis of polyester and viscose, this study aimed to promote the recycling economy of solid textile wastes, rather than discarding these products. This study provides reference information for the treatment of PET and VF textile wastes and explores a candidate approach for the reuse of textile waste resources. We will continue to investigate the synergy and catalytic activity between various textile fibers in future research, a critical step for the recycling of textile wastes.

Supplementary Information The online version contains supplementary material available at https://doi.org/10.1007/s10973-022-11521-2.

Acknowledgements This work was financially supported by the National Natural Science Foundation of China [No. 51721091].

Declaration

Conflict of interest The authors declare no conflicts of interest regarding this article.

References

1. Hanoğlu A, Çay A, Yanık J. Production of biochars from textile fibres through torrefaction and their characterisation. Energy. 2019;166:664–73. https://doi.org/10.1016/j.energy.2018.10.123.
2. Haslinger S, Hummel M, Anghelescu-Hakala A, Määttänen M, Sixta H. Upcycling of cotton polyester blended textile waste to new man-made cellulose fibers. Waste Manag. 2019;97:88–96. https://doi.org/10.1016/j.wasman.2019.07.040.
3. Nørup N, Pihl K, Damgaard A, Scheutz C. Quantity and quality of clothing and household textiles in the Danish household waste. Waste Manag. 2019;87:454–63. https://doi.org/10.1016/j.wasman.2019.02.020.
4. Subramanian K, Chopra SS, Cakin E, Li X, Lin CSK. Environmental life cycle assessment of textile bio-recycling—valorizing cotton-polyester textile waste to pet fiber and glucose syrup. Resour Conserv Recycl. 2020;161: 104989. https://doi.org/10.1016/j.resconrec.2020.104989.

5. Prata JC, Godoy V, da Costa JP, Calero M, Martín-Lara MA, Duarte AC, et al. Microplastics and fibers from three areas under different anthropogenic pressures in Douro river. Sci Total Environ. 2021;776: 145999. https://doi.org/10.1016/j.scitotenv.2021.145999.
6. Treilles R, Cayla A, Gaspéri J, Strich B, Ausset P, Tassin B. Impacts of organic matter digestion protocols on synthetic, artificial and natural raw fibers. Sci Total Environ. 2020;748: 141230. https://doi.org/10.1016/j.scitotenv.2020.141230.
7. Mintenig SM, Löder MGJ, Primpke S, Gerdts G. Low numbers of microplastics detected in drinking water from ground water sources. Sci Total Environ. 2019;648:631–5. https://doi.org/10.1016/j.scitotenv.2018.08.178.
8. Jabbar M, Shaker K. Textile raw materials. Phys Sci Rev. 2019;1:1–12. https://doi.org/10.1515/psr-2016-0022.
9. Sayyed AJ, Deshmukh NA, Pinjari DV. A critical review of manufacturing processes used in regenerated cellulosic fibres: viscose, cellulose acetate, cuprammonium, LiCl/DMAc, ionic liquids, and NMMO based lyocell. Cellulose. 2019;26:2913–40. https://doi.org/10.1007/s10570-019-02318-y.
10. Agarwal R, Jassal M, Agrawal AK. Nano surface modification of poly(ethylene terephthalate) fabrics for enhanced comfort properties for activewear. J Ind Eng Chem. 2021;98:217–30. https://doi.org/10.1016/j.jiec.2021.03.050.
11. Sharma K, Khilari V, Chaudhary BU, Jogi AB, Pandit AB, Kale RD. Cotton based composite fabric reinforced with waste polyester fibers for improved mechanical properties. Waste Manag. 2020;107:227–34. https://doi.org/10.1016/j.wasman.2020.04.011.
12. Carney Almroth BM, Åström L, Roslund S, Petersson H, Johansson M, Persson NK. Quantifying shedding of synthetic fibers from textiles; a source of microplastics released into the environment. Environ Sci Pollut Res. 2018;25:1191–9. https://doi.org/10.1007/s11356-017-0528-7.
13. Lin TR, Lin TA, Lin MC, Lin YY, Lou CW, Lin JH. Using recycled high-strength polyester and Kevlar® wastes to reinforce sandwich-structured nonwoven fabric: Structural effect and property evaluation. J Clean Prod. 2020;267: 121899. https://doi.org/10.1016/j.jclepro.2020.121899.
14. Adu C, Zhu C, Jolly M, Richardson RM, Eichhorn SJ. Continuous and sustainable cellulose filaments from ionic liquid dissolved paper sludge nanofibres. J Clean Prod. 2021;280: 124503. https://doi.org/10.1016/j.jclepro.2020.124503.
15. Xu S, Qi L, Ma C. Viscose fiber hybrid composites with high strength and practicality via cross-linking with modified melamine formaldehyde resin. Mater Today Commun. 2021. https://doi.org/10.1016/j.mtcomm.2021.102093.
16. Zhu C, Richardson RM, Potter KD, Koutsomitopoulou AF, Van Duijneveldt JS, Vincent SR, et al. High modulus regenerated cellulose fibers spun from a low molecular weight microcrystalline cellulose solution. ACS Sustain Chem Eng. 2016;4:4545–53. https://doi.org/10.1021/acssuschemeng.6b00555.
17. Chen Y, Wu X, Wei J, Wu H, Fang J. Reuse polyester/cotton blend fabrics to prepare fiber reinforced composite: fabrication, characterization, and interfacial properties evaluation. Polym Compos. 2021;42:141–52. https://doi.org/10.1002/pc.25814.
18. Kai X, Yang T, Shen S, Li R. TG-FTIR-MS study of synergistic effects during co-pyrolysis of corn stalk and high-density polyethylene (HDPE). Energy Convers Manag. 2019;181:202–13. https://doi.org/10.1016/j.enconman.2018.11.065.
19. Sun C, Li C, Tan H, Zhang Y. Synergistic effects of wood fiber and polylactic acid during co-pyrolysis using TG-FTIR-MS and Py-GC/MS. Energy Convers Manag. 2019;202: 112212. https://doi.org/10.1016/j.enconman.2019.112212.
20. Chen WH, Cheng CL, Lee KT, Lam SS, Ong HC, Ok YS, et al. Catalytic level identification of ZSM-5 on biomass pyrolysis and aromatic hydrocarbon formation. Chemosphere. 2021;271: 129510. https://doi.org/10.1016/j.chemosphere.2020.129510.
21. Li K, Wang ZX, Zhang G, Cui MS, Lu Q, Yang YP. Selective production of monocyclic aromatic hydrocarbons from: Ex situ catalytic fast pyrolysis of pine over the HZSM-5 catalyst with calcium formate as a hydrogen source. Sustain Energy Fuels. 2020;4:538–48. https://doi.org/10.1039/c9se00605b.
22. Nishu LR, Rahman MM, Li C, Chai M, Sarker M, et al. Catalytic pyrolysis of microcrystalline cellulose extracted from rice straw for high yield of hydrocarbon over alkali modified ZSM-5. Fuel. 2021;285:119038. https://doi.org/10.1016/j.fuel.2020.119038.
23. Pinheiro Pires AP, Arauzo J, Fonts I, Domine ME, Fernández Arroyo A, Garcia-Perez ME, et al. Challenges and opportunities for bio-oil refining: a review. Energy Fuels. 2019;33:4683–720. https://doi.org/10.1021/acs.energyfuels.9b00039.
24. He T, Zhong Z, Zhang B. Bio-oil upgrading via ether extraction, looped-oxide catalytic deoxygenation, and mild electrocatalytic hydrogenation techniques. Energy Fuels. 2020;34:9725–33. https://doi.org/10.1021/acs.energyfuels.0c01719.
25. Merckel RD, Heydenrych MD, Sithole BB. Pyrolysis oil composition and catalytic activity estimated by cumulative mass analysis using Py-GC/MS EGA-MS. Energy. 2021;219: 119428. https://doi.org/10.1016/j.energy.2020.119428.
26. Ryu HW, Kim DH, Jae J, Lam SS, Park ED, Park YK. Recent advances in catalytic co-pyrolysis of biomass and plastic waste for the production of petroleum-like hydrocarbons. Bioresour Technol. 2020;310: 123473. https://doi.org/10.1016/j.biortech.2020.123473.
27. Liu X, Burra KRG, Wang Z, Li J, Che D, Gupta AK. Towards enhanced understanding of synergistic effects in co-pyrolysis of pinewood and polycarbonate. Appl Energy. 2021;289: 116662. https://doi.org/10.1016/j.apenergy.2021.116662.
28. Wang Z, Burra KG, Lei T, Gupta AK. Co-pyrolysis of waste plastic and solid biomass for synergistic production of biofuels and chemicals-A review. Prog Energy Combust Sci. 2021;84: 100899. https://doi.org/10.1016/j.pecs.2020.100899.
29. Lin X, Zhang Z, Wang Q. Evaluation of zeolite catalysts on product distribution and synergy during wood-plastic composite catalytic pyrolysis. Energy. 2019. https://doi.org/10.1016/j.energy.2019.116174.
30. He T, Zhong S, Liu C, Shujaa A, Zhang B. Enhancing hydrocarbon production via ex-situ catalytic co-pyrolysis of biomass and high-density polyethylene: study of synergistic effect and aromatics selectivity. Waste Manag. 2021;128:189–99. https://doi.org/10.1016/j.wasman.2021.04.058.
31. Dorado C, Mullen CA, Boateng AA. H-ZSM5 catalyzed co-pyrolysis of biomass and plastics. ACS Sustain Chem Eng. 2014;2:301–11. https://doi.org/10.1021/sc400354g.
32. Xu S, Cao B, Uzoejinwa BB, Odey EA, Wang S, Shang H, et al. Synergistic effects of catalytic co-pyrolysis of macroalgae with waste plastics. Process Saf Environ Prot. 2020;137:34–48. https://doi.org/10.1016/j.psep.2020.02.001.
33. Gurudatt K, De P, Rakshit AK, Bardhan MK. Spinning Fibers from Poly(ethylene terephthalate) Bottle-Grade Waste. J Appl Polym Sci. 2003;90:3536–45. https://doi.org/10.1002/app.12969.
34. Qiu C, Zhu K, Zhou X, Luo L, Zeng J, Huang R, et al. Influences of coagulation conditions on the structure and properties of regenerated cellulose filaments via wet-spinning in LiOH/urea solvent. ACS Sustain Chem Eng. 2018;6:4056–67. https://doi.org/10.1021/acssuschemeng.7b04429.
35. Bach Q, Chen W. Bioresource technology pyrolysis characteristics and kinetics of microalgae via thermogravimetric analysis (TGA): a state-of-the-art review. Bioresour Technol. 2017;246:88–100. https://doi.org/10.1016/j.biortech.2017.06.087.

36. Tahir MH, Mahmood MA, Çakman G, Ceylan S. Pyrolysis of oil extracted safflower seeds: product evaluation, kinetic and thermodynamic studies. Bioresour Technol. 2020. https://doi.org/10.1016/j.biortech.2020.123699.
37. Jia H, Ben H, Luo Y, Wang R. Catalytic fast pyrolysis of poly (ethylene terephthalate) (PET) with zeolite and nickel chloride. Polymers (Basel). 2020;12:1–14.
38. Bu Q, Lei H, Wang L, Wei Y, Zhu L, Zhang X, et al. Bio-based phenols and fuel production from catalytic microwave pyrolysis of lignin by activated carbons. Bioresour Technol. 2014;162:142–7. https://doi.org/10.1016/j.biortech.2014.03.103.
39. Kim YM, Han TU, Hwang BA, Lee B, Lee HW, Park YK, et al. Pyrolysis kinetics and product properties of softwoods, hardwoods, and the nut shell of softwood. Korean J Chem Eng. 2016;33:2350–8. https://doi.org/10.1007/s11814-016-0142-2.
40. Park YK, Jung J, Ryu S, Lee HW, Siddiqui MZ, Jae J, et al. Catalytic co-pyrolysis of yellow poplar wood and polyethylene terephthalate over two stage calcium oxide-ZSM-5. Appl Energy. 2019;250:1706–18. https://doi.org/10.1016/j.apenergy.2019.05.088.
41. Nishu LR, Rahman MM, Sarker M, Chai M, Li C, et al. A review on the catalytic pyrolysis of biomass for the bio-oil production with ZSM-5: focus on structure. Fuel Process Technol. 2020;199:106301. https://doi.org/10.1016/j.fuproc.2019.106301.
42. Zheng Y, Tao L, Yang X, Huang Y, Liu C, Zheng Z. Study of the thermal behavior, kinetics, and product characterization of biomass and low-density polyethylene co-pyrolysis by thermogravimetric analysis and pyrolysis-GC/MS. J Anal Appl Pyrolysis. 2018;133:185–97. https://doi.org/10.1016/j.jaap.2018.04.001.
43. Oyedun AO, Tee CZ, Hanson S, Hui CW. Thermogravimetric analysis of the pyrolysis characteristics and kinetics of plastics and biomass blends. Fuel Process Technol. 2014;128:471–81. https://doi.org/10.1016/j.fuproc.2014.08.010.
44. Wang Z, Liu G, Shen D, Wu C, Gu S. Co-pyrolysis of lignin and polyethylene with the addition of transition metals—part I: thermal behavior and kinetics analysis. J Energy Inst. 2020;93:281–91. https://doi.org/10.1016/j.joei.2019.03.003.
45. Fan H, Gu J, Hu S, Yuan H, Chen Y. Co-pyrolysis and co-gasification of biomass and polyethylene: thermal behaviors, volatile products and characteristics of their residues. J Energy Inst. 2019;92:1926–35. https://doi.org/10.1016/j.joei.2018.11.002.
46. Han B, Chen Y, Wu Y, Hua D, Chen Z, Feng W, et al. Co-pyrolysis behaviors and kinetics of plastics-biomass blends through thermogravimetric analysis. J Therm Anal Calorim. 2014;115:227–35. https://doi.org/10.1007/s10973-013-3228-7.
47. Park YK, Lee B, Lee HW, Watanabe A, Jae J, Tsang YF, et al. Co-feeding effect of waste plastic films on the catalytic pyrolysis of Quercus variabilis over microporous HZSM-5 and HY catalysts. Chem Eng J. 2019;378: 122151. https://doi.org/10.1016/j.cej.2019.122151.
48. Buxbaum BYLH. The degradation of poly (ethy1ene terephthalate). Angew Chem internat Ed. 1968;7:182–90.
49. Yang H, Huan B, Chen Y, Gao Y, Li J, Chen H. Biomass-based pyrolytic polygeneration system for Bamboo industry waste: evolution of the char structure and the pyrolysis mechanism. Energy Fuels. 2016;30:6430–9. https://doi.org/10.1021/acs.energyfuels.6b00732.
50. Zhang B, Zhong Z, Ding K, Song Z. Production of aromatic hydrocarbons from catalytic co-pyrolysis of biomass and high density polyethylene: analytical Py-GC/MS study. Fuel. 2015;139:622–8. https://doi.org/10.1016/j.fuel.2014.09.052.
51. Lin X, Zhang Z, Zhang Z, Sun J, Wang Q, Pittman CU. Catalytic fast pyrolysis of a wood-plastic composite with metal oxides as catalysts. Waste Manag. 2018;79:38–47. https://doi.org/10.1016/j.wasman.2018.07.021.
52. Lee HW, Kim YM, Lee B, Kim S, Jae J, Jung SC, et al. Catalytic copyrolysis of torrefied cork oak and high density polyethylene over a mesoporous HY catalyst. Catal Today. 2018;307:301–7. https://doi.org/10.1016/j.cattod.2017.01.036.
53. Zhang H, Carlson TR, Xiao R, Huber GW. Catalytic fast pyrolysis of wood and alcohol mixtures in a fluidized bed reactor. Green Chem. 2012;14:98–110. https://doi.org/10.1039/c1gc15619e.
54. Du S, Gamliel DP, Giotto MV, Valla JA, Bollas GM. Coke formation of model compounds relevant to pyrolysis bio-oil over ZSM-5. Appl Catal A Gen. 2016;513:67–81. https://doi.org/10.1016/j.apcata.2015.12.022.
55. Foster AJ, Jae J, Cheng YT, Huber GW, Lobo RF. Optimizing the aromatic yield and distribution from catalytic fast pyrolysis of biomass over ZSM-5. Appl Catal A Gen. 2012;423–424:154–61. https://doi.org/10.1016/j.apcata.2012.02.030.